THE JOURNAL OF BIOLOGICAL CHEMISTRY VOL. 282, NO. 14, pp. 10605–10613, April 6, 2007

Loading of the Nonhomologous End Joining Factor, Ku, on Protein-occluded DNA Ends*

Received for publication, December 4, 2006, and in revised form, February 6, 2007 Published, JBC Papers in Press, February 8, 2007, DOI 10.1074/jbc.M611125200

Steven A. Roberts and Dale A. Ramsden[1]

From the Lineberger Comprehensive Cancer Center and Department of Biochemistry and Biophysics, University of North Carolina at Chapel Hill, Chapel Hill, North Carolina 27599

The nonhomologous end joining pathway for DNA double strand break repair requires Ku to bind DNA ends and subsequently recruit other nonhomologous end joining factors, including the DNA-dependent protein kinase catalytic subunit and the XRCC4-Ligase IV complex, to the break site. Ku loads at a break by threading the DNA ends through a circular channel in its structure. This binding mechanism explains both the high specificity of Ku for ends and its ability to translocate along DNA once loaded. However, DNA in cells is typically coated with other proteins (*e.g.* histones), which might be expected to block the ability of Ku to load in this manner. Here we address how the nature of a protein obstruction dictates how Ku interacts with a DNA end. Ku is unable to access the ends within an important intermediate in V(D)J recombination (a complex of RAG proteins bound to cleaved recombination targeting signals), but Ku readily displaces the linker histone, H1, from DNA. Ku also retains physiological affinity for nucleosome-associated ends. Loading onto nucleosome-associated ends still occurs by threading the end through its channel, but rather than displacing the nucleosome, Ku peels as much as 50 bp of DNA away from the histone octamer surface. We suggest a model where Ku utilizes an unusual characteristic of its three-dimensional structure to recognize certain protein-occluded ends without the extensive remodeling of chromatin structure required by other DNA repair pathways.

DNA double strand breaks (DSBs)[2] pose a threat to genomic integrity. Nonhomologous end joining (NHEJ) is a major pathway for repair of exogenously introduced DSBs in mammals and is the only efficient way to repair DSB intermediates in V(D)J recombination (1). NHEJ requires the DNA binding heterodimer Ku to first recognize broken DNA ends (2–5) and subsequently recruit the additional NHEJ factors necessary to complete repair (*e.g.* DNA-dependent protein kinase catalytic subunit (DNA-PKcs) (6), the XRCC4-LigaseIV complex (7, 8), and polymerases (9, 10)). Consequently, deficiency in Ku cripples NHEJ and leads to severe immunodeficiency (11, 12) and cellular sensitivity to agents that cause DSBs (*e.g.* ionizing radiation) (13, 14). The ability of Ku to recognize DNA ends requires the end to be inserted through a channel in its structure (5, 15, 16). This manner of binding makes Ku highly specific for DNA ends but requires that the ends must be accessible through 360°. In cells, DNA is generally coated with proteins (*e.g.* histones and other chromatin-associated proteins) that might be expected to block the ability of Ku to load on DNA ends and thus impair NHEJ.

Here we have shown that Ku displays a variety of responses to protein obstructions at DNA ends. Ku is unable to bind a class of RAG (recombination activating gene) protein-bound DNA ends generated during V(D)J recombination. In contrast, Ku can displace certain proteins (*e.g.* histone H1) from DNA and retains the ability to load on nucleosome-associated ends by peeling up to 50 bp of DNA away from the nucleosome surface. We therefore suggest Ku may be specifically suited to loading on protein-obstructed DNA ends, ultimately facilitating the recruitment of the NHEJ machinery without requiring extensive remodeling of chromatin structure at broken ends.

EXPERIMENTAL PROCEDURES

Purified Proteins—Bulk histones were purified from 5 liters of HeLa cells as described previously (17). Briefly, a nuclear pellet was isolated and homogenized, and genomic DNA was sheared by sonication. The clarified supernatant was then applied to a hydroxyapatite column equilibrated in 0.6 M NaCl. The column was washed extensively with the equilibration buffer to deplete linker histones and non-histone proteins, and fractions primarily containing core histones were eluted with 2 M NaCl. This eluent was then applied to a S200 gel filtration column equilibrated in 2 M NaCl to further deplete linker histones and ensure the proper stoichiometry of the core histone octamer. Histone H1 was a gift from Dr. Yi Zhang. Recombinant core RAG1 and RAG2 maltose-binding protein fusions and recombinant Ku were obtained as previously described in Refs. 18 and 7, respectively.

DNA Substrates—DNA duplexes used in the histone H1 and RAG electrophoretic mobility shift assays (EMSAs) (Figs. 1 and 7) were generated by T4 polynucleotide kinase labeling an oligonucleotide with [γ-^{32}P]ATP and annealing it to a complementary oligonucleotide. The 23-recombination signal (RS)

* This work was supported by United States Public Health Service Grant CA-84442 (to D. A. R.). The costs of publication of this article were defrayed in part by the payment of page charges. This article must therefore be hereby marked "*advertisement*" in accordance with 18 U.S.C. Section 1734 solely to indicate this fact.

[1] A Leukemia and Lymphoma Society Scholar. To whom correspondence should be addressed: Lineberger Comprehensive Cancer Center and Dept. of Biochemistry and Biophysics, University of North Carolina at Chapel Hill, CB-7295, Chapel Hill, NC 27599. Tel.: 919-966-9839; Fax: 919-966-3015; E-mail: dale_ramsden@med.unc.edu.

[2] The abbreviations used are: DSB, double strand break; NHEJ, nonhomologous end joining; DNA-PKcs, DNA-dependent protein kinase catalytic subunit; XRCC4, X-ray cross-complementary gene 4; RAG, recombination activation gene; EMSA, electrophoretic mobility shift assay; RS, recombination signal; SEC, paired signal end complex; HMG1, high mobility group protein 1; MOPS, 4-morpholinepropanesulfonic acid.

duplex, 12-RS duplex, and histone H1 EMSA substrate consist of the following paired oligonucleotides, respectively: 5′-CACAGTGGTAGTACTCCACTGTCTGGCTGTACAAAAACCCTCGGGACG and biotin-tetraethyleneglycol-5′-CGTCCCGAGGGTTTTTGTACAGCCAGACAGTGGAGTACTACCACTGTG, 5′-CACAGTGCTACAGACTGGAACAAAAACCCTGCAGACG and biotin-tetraethyleneglycol-5′-CGTCTGCAGGGTTTTTGTTCCAGTCTGTAGCACTGTG, and finally 5′-ATGGAAATTGTGAGCGGATAACAATTCAATG and 5′-CATTGAATTGTTATCCGCTCACAATTTCCAT. The 601.2-nucleosome positioning sequence (19, 20) was obtained from Dr. Jonathon Widom and inserted into the EcoR1 and NheI sites of the litmus 38 (New England Biolabs) multiple cloning region. This plasmid served as a template for PCR with the primers 5′-CTGCAGAAGCTTGGTCCCG and 5′-ACAGGATGTATATATCTGACACG to generate unlabeled DNA for core nucleosomes (Fig. 2) or with the primers biotin-tetraethyleneglycol-5′-GATATCTGGATCCACGAATTC and 5′-ACAGGATGTATATATCTGACACG in the presence of [α-^{32}P]dCTP to generate the radiolabeled DNA for nucleosomes containing a 40-bp linker (Figs. 3, *B* and *C*, 4, 5*A* (without [α-^{32}P]dCTP), and 6*D*). Nucleosomes used in footprinting experiments (Fig. 6, *A*–*C*) were labeled by substituting the biotinylated primer described above with the fluorescent biotinylated primer biotin-decaethyleneglycol-bodipy 630–5′-GATATCTGGATCCACGAATTC (Integrated DNA Technologies).

Nucleosomes—As described previously (21), nucleosomes were reconstituted on positioning sequences by salt dialysis using a DNA to histone ratio determined empirically for each DNA preparation such that reconstitutions contained less than 5% free DNA. The quality of reconstitutions was monitored by EMSA. Nucleosomes used for footprinting were also purified by preparative electrophoresis using a Mini-prep cell (Bio-Rad) (22). Native mononucleosomes were obtained by resuspending HeLa nuclei in 10 ml of micrococcal nuclease digestion buffer (10 mM Tris, pH 7.5, 5 mM $MgCl_2$, 5 mM $CaCl_2$, 0.1 mM phenylmethylsulfonyl fluoride, and 0.5 mM dithiothreitol) and digestion with 0.02 units/μl of micrococcal nuclease (USB) at 37 °C for 8 min (17). After addition of NaCl to 0.6 M, the suspension was dounced to extract soluble chromatin and subsequently pelleted. The resulting supernatant was separated on a 5–30% sucrose gradient. As mononucleosomes derived from this digestion are rich in linker histones (17), we excluded mononucleosome-containing fractions and further digested pooled oligonucleosome-containing fractions with 1.5 units/μl micrococcal nuclease at 0 °C for 40 min to generate core mononucleosomes. Mononucleosomes were further purified on a second sucrose gradient.

EMSA—DNA-protein complexes were assembled prior to EMSA by incubation of the DNA and proteins in a standard reaction buffer (10 mM Tris, pH 7.5, 145 mM NaCl, 0.5 mg/ml bovine serum albumin, 1 mM dithiothreitol, 0.1 mM EDTA), except for experiments using the signal end complex (SEC), which used the following buffer: 25 mM MOPS, pH 7, 120 mM KCl, 5 mM $CaCl_2$, 0.1 mg/ml bovine serum albumin, 2 mM dithiothreitol, and 0.125 ng/μl of supercoiled DNA plasmid. The resulting complexes were resolved by electrophoresis at 300 V for 1 h through a 16-cm, 1/3× Tris borate-EDTA, 3.5% polyacrylamide gel containing 100 μg/ml bovine serum albumin. EMSAs containing antibody supershifts used the following antibodies: α-Ku (Ab-3; Neomarkers), α-MBP (New England Biolabs), and α-histone H1 (clone B419; Biomeda) purified by batch adsorption with hydroxyapatite beads.

In Fig. 4, the apparent dissociation constant (K_d) was calculated from quantified (using ImageQuant; GE Healthcare) EMSA experiments according to the equation, $K_d = [Ku_{free}]^*[DNA_{free}]/[Ku{:}DNA]$.

When 50% of the substrate is bound, $[Ku{:}DNA] = [DNA_{free}]$, thus $K_d = [Ku_{free}]$. Because the total amount of Ku was kept in large excess over total DNA (>40-fold for experiments in Fig. 4) and $[Ku_{free}] = [Ku_{total}] - [Ku{:}DNA]$, $[Ku_{free}]$ was further approximated as $[Ku_{total}]$ (also see Ref. 23). The fraction-shifted species (determined from EMSAs) was plotted against the log of Ku's concentration. The resulting binding curves were best fit with a sigmoidal dose-response (variable slope) regression line (GraphPad Prism version 4.03 (Trial) for Windows, GraphPad Software, San Diego CA) to determine apparent K_ds and associated error.

Analysis of the Protein Composition of Ku-Nucleosome Complexes—Large-scale 50-μl EMSA reactions were generated by incubating 80 nM nucleosome or free DNA with either 60, 120, or 240 nM Ku in our standard EMSA buffer at 25 °C for 10 min. Reactions were then incubated for 5 min at 37 °C before separating the formed complexes as described above. Ku-nucleosome and Ku-DNA complexes were visualized by ethidium bromide staining and subsequently excised. Complexes were then electro-eluted from the gel and their protein components concentrated by trichloroacetic acid precipitation. The relative amounts of Ku and histone H3 in each of the excised complexes were determined by semi- quantitative Western analysis probing with a polyclonal rabbit antibody raised against native, recombinant human Ku and a polyclonal antibody against histone H3 (Ab1791; Abcam) using fluorescent detection and a Typhoon imager (GE Healthcare). Western blots were quantified using ImageQuantTL (GE Healthcare), and the ratio of Ku70 (Ku80 is overexposed) to H3 was determined for nucleosome-containing complexes (Fig. 5*B*, *species IV*, *V*, and *VI*).

Hydroxyl Radical Footprinting—Footprinting experiments utilize an asymmetrically positioned nucleosome substrate containing a single 40-bp linker DNA (24). The DNA end of this linker was labeled with a bodipy 630 fluorophore (Integrated DNA Technologies) and blocked with a biotin-streptavidin complex (Fig. 6*A*). Footprinting reactions were conducted in 15 μl of 30 mM Tris, pH 8.0, and 0.1 mM EDTA by incubating 80 nM nucleosome with 120 or 240 nM Ku at 25 °C for 10 min. Reactions were then incubated at 37 °C for 5 min before being placed on ice. Nucleosomes were twice treated at 4 °C with 3.5 μl of 3% hydrogen peroxide, 3.5 μl of a 2-mM ammonium iron(II) sulfate and 4 mM EDTA mixture, and 3.5 μl of 20 mM sodium ascorbate at 5-min intervals before reactions were stopped by addition of 5 μl of 400 mM thiourea (24). Reactions were acidified by addition of 5 μl of 3 M sodium acetate, and nicked DNA was purified through a minElute reaction clean-up column (Qiagen). Eluted DNA was electrophoresed on an 8% urea-PAGE sequencing gel at 1800 V and 40 watts for either 1.5 (Fig. 6*B*) or 4 h (Fig. 6*C*).

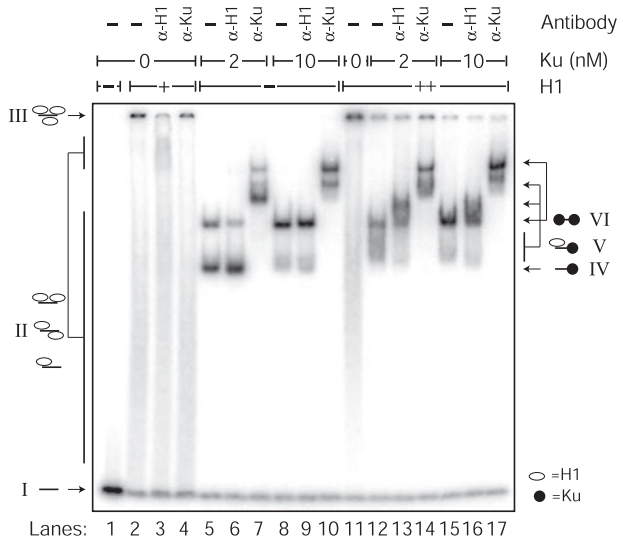

FIGURE 1. **The DNA binding activity of Ku at H1 bound DNA ends.** Increasing concentrations of Ku (0, 2, 10 nM) were incubated for 10 min at 25 °C with 1 nM 31-bp DNA duplex (*lanes 1* and *5–10*) or the same duplex prebound for 10 min at 25 °C with 100 nM histone H1 (*lanes 2–4*) or 500 nM H1 (*lanes 11–17*). The presence of Ku or H1 in various species was confirmed by supershift with an α-Ku antibody (*lanes 4*, *7*, *10*, *14*, *17*) or α-H1 antibody (*lanes 3*, *6*, *9*, *13*, *16*). The compositions of DNA protein complexes were inferred from relative mobilities and antibody supershifts as noted at the sides of the panel: *species I*, naked DNA duplex; *species II*, heterogeneous complexes of H1 bound to DNA; *species III*, H1 saturated DNA; *species IV*, DNA bound by one molecule of Ku; *species V*, DNA bound by Ku and H1; *species VI*, DNA bound by two molecules of Ku. Antibody supershifts are denoted as the *upper arrows* within a bracket.

Protein Modeling—The SPOCK modeling program (25) was used to dock the crystal structures of the core nucleosome (Protein Data Bank accession 1AOI) and Ku bound to DNA (accession 1JEY) by multiple alignments of the phosphodiester backbone of residues 2–12 in chain C of 1JEY with the backbone of 10 consecutive residues in chain I of 1AOI. Iterative alignments were made, advancing target phosphate positions in the nucleosome in single nucleotide steps, until steric clashes were minimized to generate the docked structure model shown in Fig. 8, where residues 2–12 in chain C of 1JEY are aligned with residues 10–20 in chain I of 1AOI.

RESULTS

Ku Displaces Histone H1 from DNA Ends—Binding of protein to DNA fragments has been shown *in vitro* to inhibit the ability of XRCC4-Ligase IV to join DNA ends (26, 27). Interestingly, Ku and DNA-PKcs are required to relieve the specific inhibition caused by the presence of the linker histone H1 (27), suggesting Ku may play roles in recognizing H1-occluded DNA ends and making these ends accessible to DNA-PKcs and XRCC4-ligase IV. To address this possibility, we incubated a radiolabeled 31-bp DNA duplex with a large excess (500-fold) of the linker histone. This generates H1-DNA complexes with heterogeneous mobility (Fig. 1, *lane 11*), including aggregates that remain in the well (species III). Addition of Ku to these reactions results in progressive redistribution of the H1-bound DNA into two species (species V and VI). Species V is heterogenous, and its mobility can be reduced by antibodies to either H1 or Ku, indicative of the presence of at least one molecule of both. Species VI is more abundant at higher concentrations of Ku and is consistent with DNA where Ku has mostly evicted

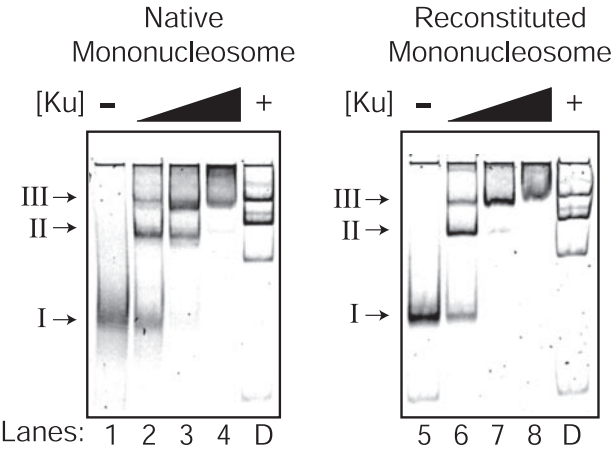

FIGURE 2. **The DNA binding activity of Ku at nucleosome-associated ends.** 10 nM HeLa-derived core mononucleosomes (*lanes 1–4*), reconstituted core mononucleosomes (*lanes 5–8*), or 147-bp naked DNA (*lanes marked D*) were incubated with 50 nM Ku (*lanes 2*, *6*, and *D*), 100 nM Ku (*lanes 3* and *7*), or 200 nM Ku (*lanes 4* and *8*) for 10 min at 25 °C. The resulting complexes were separated by gel electrophoresis and visualized by SYBR Green staining. *Roman numerals* indicate various Ku-bound species as described under "Results."

H1; the mobility of a large proportion of this species resists addition of the α-H1 antibody, and its mobility is equivalent to DNA saturated by Ku only (compare *lanes 8–10* to *15–17*). Eviction of H1 occurs even when the Ku concentration is one-fiftieth the concentration of H1. Ku is thus remarkably effective at clearing DNA of histone H1.

Ku Threads on Nucleosome-associated DNA Ends—We next addressed whether the ability of Ku to load on H1-occluded ends could be generalized to other physiologically relevant protein-DNA complexes. The nucleosome is the protein occlusion that Ku is most likely to encounter near a DSB produced by exogenous DNA-damaging agents (*e.g.* ionizing radiation). We therefore addressed whether Ku could load on DNA ends in the context of "linker-less" mononucleosomes purified from bulk cellular chromatin (Fig. 2, *species I*). To obtain these core nucleosomes, oligonucleosome fragments lacking linker histones were first purified by sucrose gradient and subsequently subjected to exhaustive micrococcal nuclease digestion, generating a mononucleosome containing 147 bp of DNA (17)[3]. We then assessed whether Ku could bind these mononucleosomes by EMSA. Consistent with previous reports (5, 28), incubation of Ku with either native or reconstituted mononucleosomes shifts the mobility of the nucleosome in a manner dependent on Ku concentration (Fig. 2, *species II* and *III*), arguing Ku binds to nucleosome-associated ends.

Given the way Ku loads on naked DNA ends (threading of ends through a central channel), Ku must either have altered how it binds DNA ends or loading of Ku involves some form of nucleosome remodeling. We employed a series of homogeneously positioned mononucleosome substrates (*e.g.* Figs. 2 and 3) and a previously described end-blocking strategy (15, 29) to address this issue in greater detail. Ku can bind if one but not both ends of a naked DNA fragment are blocked by terminal biotin-streptavidin complexes (Fig. 3*A*). We therefore reconstituted singly positioned mononucleosomes containing biotin

[3] S. A. Roberts and D. A. Ramsden, unpublished data.

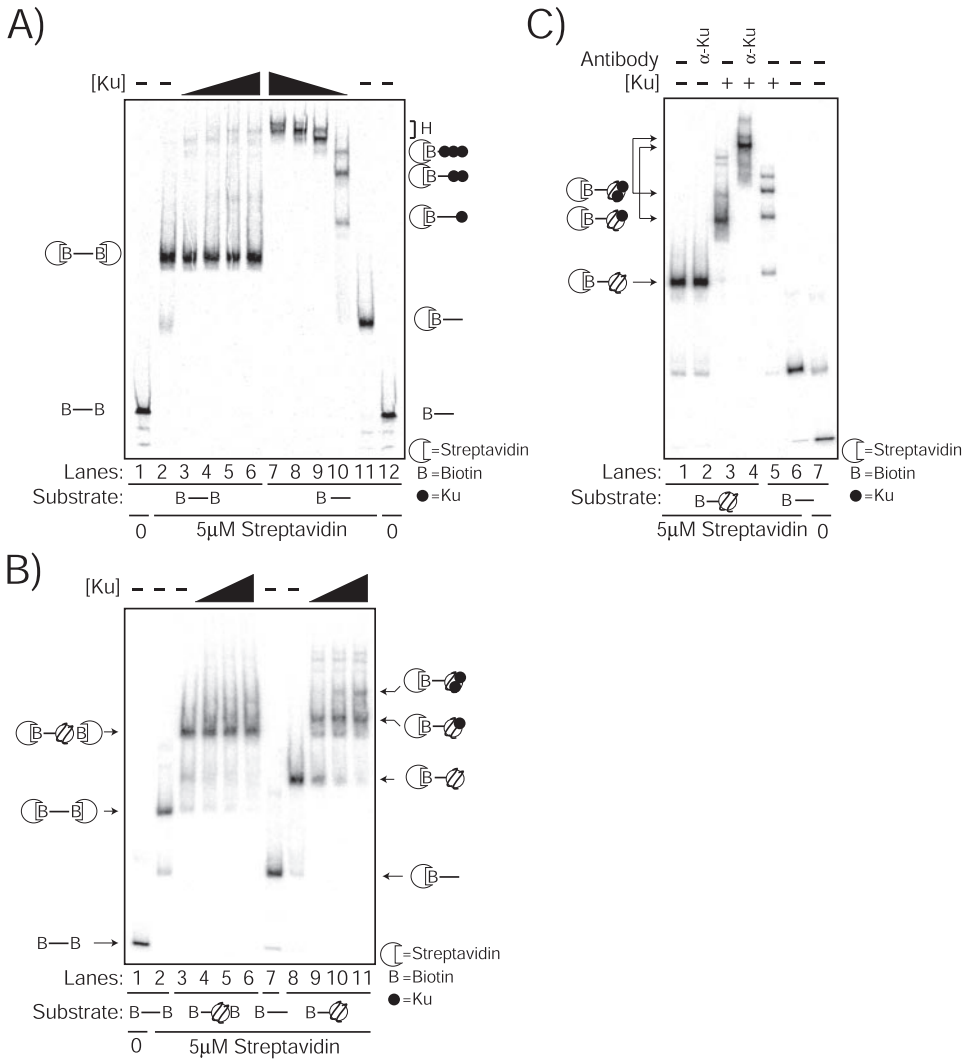

FIGURE 3. **Assessment of the ability of Ku to thread on nucleosome-associated DNA ends.** DNA substrates containing a biotin at one or both DNA ends (as indicated) were incubated with 5 μM streptavidin (except as noted) at 25 °C for 5 min. *A*, 10 pM naked DNA substrate was incubated at 25 °C for 10 min without Ku (*lanes 1–2* and *11–12*) or with 0.5 nM (*lanes 3* and *10*), 1 nM (*lanes 4* and *9*), 2 nM (*lanes 5* and *8*), or 4 nM (*lanes 6* and *7*) Ku. *B*, as in *panel A*, except using reconstituted nucleosomes incubated with 10 nM (*lanes 4* and *9*), 20 nM (*lanes 5* and *10*), or 30 nM (*lanes 6* and *11*) Ku and containing an additional 20-min 37 °C incubation. *C*, as in *panel B* except nucleosomes were incubated with 50 nM Ku (*lanes 3* and *4*) and an α-Ku antibody (*lanes 2* and *4*). *Lanes 5–7* contain the corresponding naked DNA substrate incubated with (*lane 5*) or without (*lanes 6* and *7*) 1 nM Ku. The inferred compositions of various species are noted at the side of each panel. In *panel A*, *H* indicates DNA duplexes bound by more than three molecules of Ku.

appended to one or both DNA ends. Importantly, as with naked DNA, Ku requires at least one unblocked end before it can shift the equivalent nucleosome substrate (Fig. 3*B*). Antibodies to Ku further reduced the mobility of candidate Ku-bound nucleosome species, confirming Ku is stably retained in these species (Fig. 3*C*). Ku thus loads on nucleosome-associated DNA ends the same way it loads on naked DNA, by threading DNA ends through its channel.

The singly blocked nucleosome substrate was then used to determine the extent to which nucleosome association reduces the affinity of Ku for DNA ends. In accordance with previous estimates (2, 23), Ku displays an apparent K_d of 0.34 ± 0.02 nM for the first molecule binding a naked DNA end (Fig. 4*A*). However, when confronted with ends on the surface of a nucleosome, Ku binds with an apparent K_d of 6.0 ± 0.4 nM for the first Ku bound (Fig. 4*B*). Ku is thus somewhat less able to load on nucleosome-associated ends but nevertheless retains an affinity for nucleosome-associated DNA ends that is comparable with the affinity of other DNA-binding proteins for naked DNA (*e.g.* ~3 nM for HMG1 and ~1 μM for Rad51) (30–32).

Once bound, Ku can translocate internally on linear DNA, allowing successive molecules of Ku to load on the same DNA end (33). In EMSA experiments, this appears as "ladder" of distinct species of reduced mobility, each with an additional molecule of Ku (Fig. 3*A* and Refs. 5 and 33). Multiple species are similarly observed upon addition of Ku to nucleosome-associated ends (Fig. 3*B*, *lanes 10* and *11*, Fig. 5*A*, *lane 10*). We purified these species and determined their protein complement by semi-quantitative Western analysis (Fig. 5*B*). Ku and a representative histone (H3) are present in each species as appropriate. Additionally, the ratio of Ku to histone in species VI is 2.1 times that of species V, consistent with the presence of one and two molecules of Ku per nucleosome-associated end in the two respective species. Significantly, while each molecule of Ku loads on naked DNA ends essentially independently of prior molecules loaded (Fig. 4*A* and Ref. 34), the nucleosome strongly resists loading of a second molecule of Ku (K_d of second molecule >25 nM; Fig. 4*B*).

Ku Peels DNA Ends from the Nucleosome Surface—The ability of Ku to bind nucleosome-associated DNA ends and even translocate internally to some extent indicates Ku must alter nucleosome structure in some manner. We considered three possibilities: Ku could reposition the histone octamer away from the DNA end ("pushing"), Ku could leave the nucleosome in its initial position and "peel" the DNA end away from the octamer surface, or Ku could evict a subset of core histones near the DNA end. To address these possibilities, we generated a 187-bp substrate with the nucleosome positioned at one DNA end, leaving the other DNA end spaced 40 bps from the histone octamer (*e.g.* as in Ref. 24). This end distal to the nucleosome was also blocked with a biotin-streptavidin complex, thereby forcing Ku to load from the nucleosome-associated end (Fig. 6*A*). Hydroxyl radical footprinting of this substrate shows a 10-bp phasing indicative of a

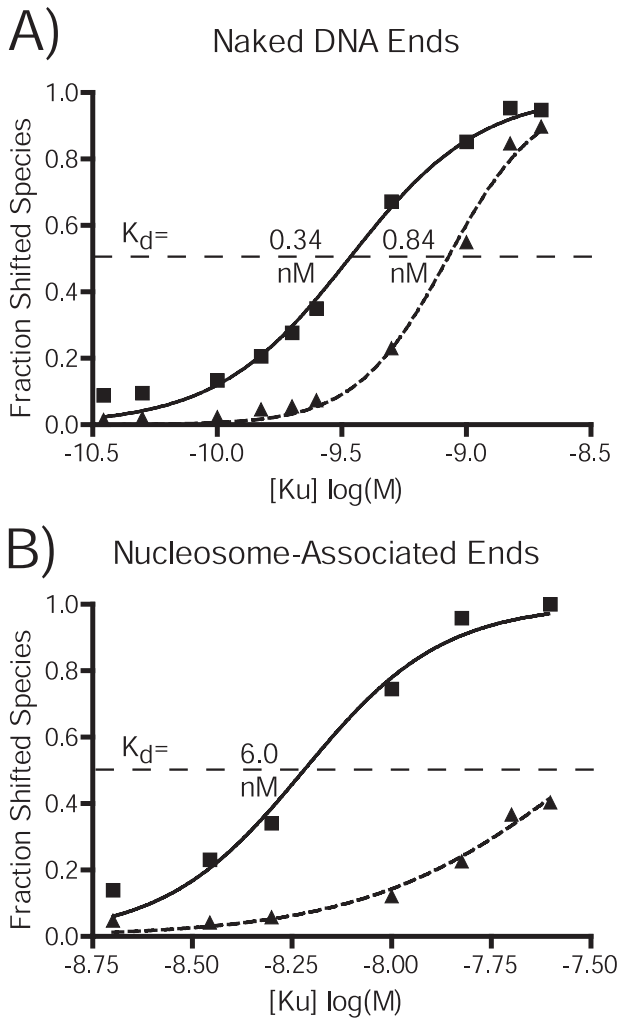

FIGURE 4. **Affinity of Ku for nucleosome-associated DNA ends.** The fraction of species with one Ku bound (*squares*) or more than one Ku bound (*triangles*; see also Fig. 5) was determined for various concentrations of Ku (50 pM-25 nM) incubated at 25 °C for 10 min and then 37 °C for 20 min with 10 pM naked DNA (*A*) or reconstituted nucleosome (*B*). As described under "Experimental Procedures," the noted K_ds were approximated, after curve fitting, as the amount of Ku required to bind 50% of substrate.

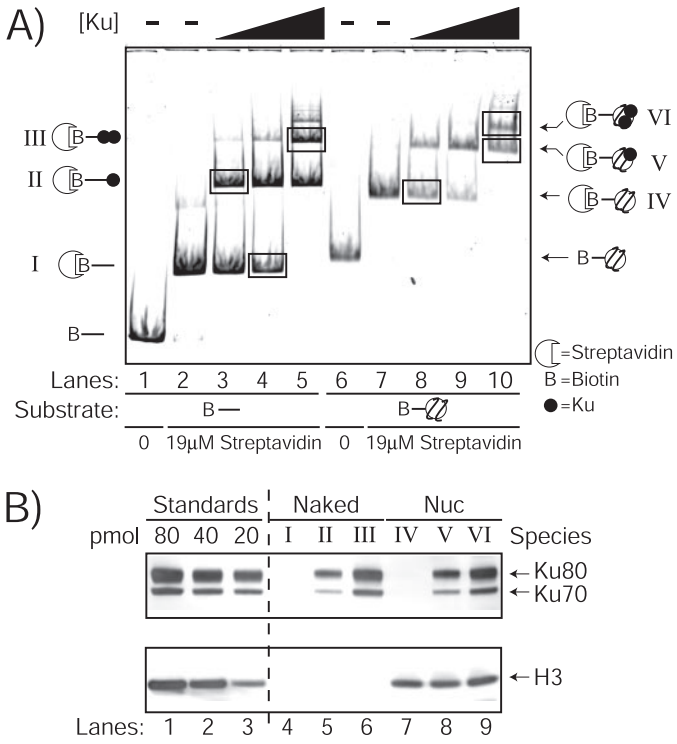

FIGURE 5. **Analysis of the protein composition of Ku-shifted species.** *A*, 80 nM singly blocked naked DNA (*lanes 1–5*) or nucleosome substrates (*lanes 6–10*) were incubated with 60 nM (*lanes 3* and *8*), 120 nM (*lanes 4* and *9*), or 240 nM (*lanes 5* and *10*) Ku at 25 °C for 10 min. Reactions were then incubated at 37 °C for 5 min before separating the formed complexes by polyacrylamide gel electrophoresis. Complexes were visualized by ethidium bromide staining, and the species of interest were excised as indicated with *boxes*. *B*, in *lanes 4–9*, the protein complements of species gel-purified in *panel A* (labeled *I–VI*) were analyzed by Western blotting using α-Ku and α-histone H3 antibodies (as indicated to the right of the panel) after electro-elution, precipitation, and SDS-PAGE. In *lanes 1–3* (*Standards*), 80, 40, and 20 pmol of Ku or nucleosome (*e.g.* H3 dimer) were loaded directly to verify the Western is semi-quantitative.

nucleosome positioned at the Ku-accessible DNA end (Fig. 6*B*, *lane 1*, *top of lane to PstI marker*). If loading of Ku on the open DNA end were to push the nucleosome onto the 40 bps of naked "linker" DNA, the phased hydroxyl radical sensitivity would either be shifted away from the end (if all nucleosomes in the sample were homogeneously pushed) or lost over the entire length of the substrate (if the nucleosomes were pushed various distances). Alternatively, DNA peeling would be apparent as a loss of phasing limited to the region near the accessible DNA end.

Addition of Ku to our footprinting reactions has a general quenching effect, resulting in an overall reduction of hydroxyl radical cleavage (Fig. 6*B*). To account for this, we included a control substrate where both DNA ends are blocked with biotin-streptavidin complexes (Fig. 6, *B* and *C*, *lanes 4*). Our data show that even at high concentrations of Ku, there are no major changes in hydroxyl radical sensitivity of the linker DNA (0–40 bps away from the label) or in the pattern of the phasing over most of the nucleosome (40 to ~140 bps from the label) (Fig. 6, *B* and *C*, compare *lanes 3* and *4*). We therefore conclude that in the majority of molecules, loading of Ku does not alter the translational location of the nucleosome on this DNA fragment.

However, increasing concentrations of Ku result in a correlating loss of phases near the accessible end, consistent with Ku peeling the DNA end away from the surface of the nucleosome. As expected, the phasing pattern of the doubly blocked nucleosome in this region is resistant to addition of Ku (Fig. 6*C*, compare *lanes 3* and *4*). When Ku is present at 3-fold excess over the nucleosome, loss of phasing extends over the first 40 bp, with some protection observed as much as 50 bp (one-third of the length of the nucleosome) away from the end. Parallel experiments indicate the majority of nucleosome substrate possesses more than one molecule of Ku under these conditions (Fig. 5, *lane 10*), arguing a molecule of Ku is able to load and translocate internally 40–50 bp, allowing a second molecule to load. Thus, Ku displays the unique ability to thread on nucleosome-associated DNA ends, gaining access to the DNA end by a peeling mechanism.

It is possible that the nucleosome accommodates loading of Ku through displacement of some subset of core histones. To address this possibility, we first loaded Ku onto nucleosome-associated ends and then added a large excess of linear compet-

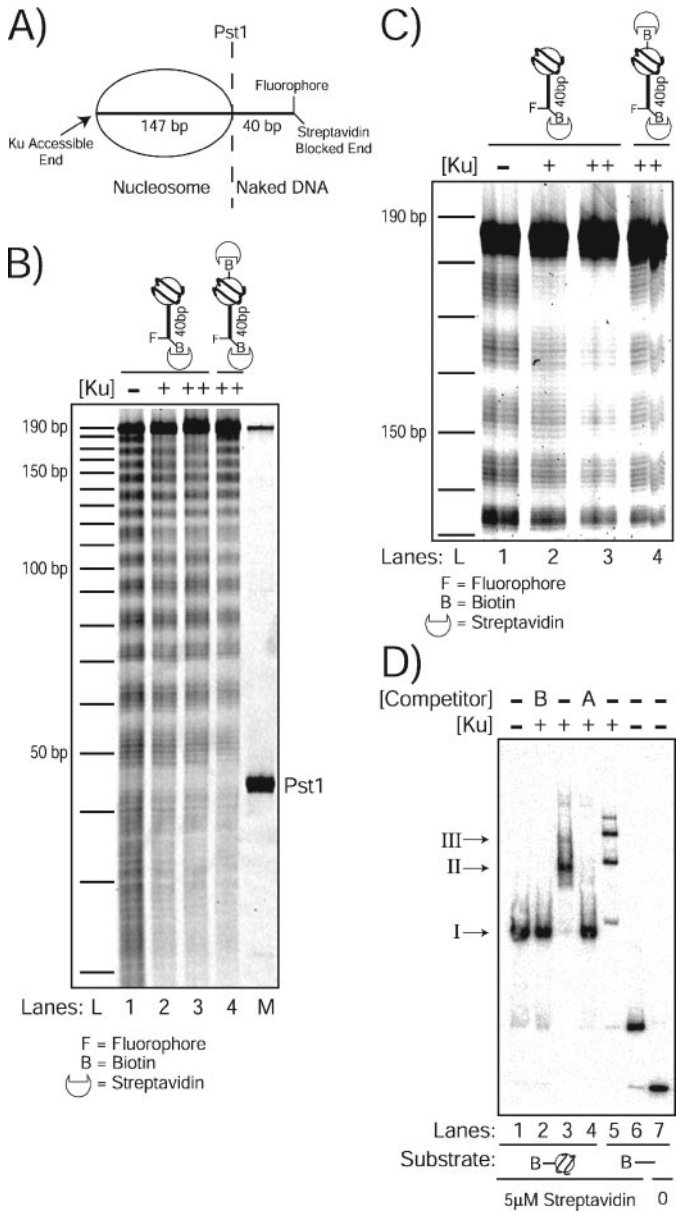

FIGURE 6. **Hydroxyl radical footprinting of nucleosomes in the presence of Ku.** *A*, the footprinting substrate consists of a 187-bp DNA fragment where the previously described positioning sequence locates the nucleosome at one end, leaving a 40-bp linker of naked DNA whose end is fluorescently labeled and blocked by a biotin-streptavidin complex. PstI digestion produces a 40-bp fragment that marks the boundary between the nucleosome and naked DNA (*panel B*, *lane M*). *B* and *C*, 80 nM singly (*lanes 1–3*) or doubly (*lane 4*) blocked nucleosomes were incubated with 0 nM (*lane 1*), 120 nM (*lane 2*), or 240 nM Ku (*lanes 3–4*) at 25 °C for 10 min followed by a 5-min 37 °C incubation. Reactions were placed on ice, treated as described under "Experimental Procedures," and electrophoresed for either 1.5 (*B*) or 4 h (*C*). *Lane L* represents the mobility of a Cy5-labeled 10-bp ladder. *D*, 30 nM Ku was incubated with 10 pM nucleosome (*lanes 1–4*) and 1 nM Ku incubated with naked DNA (*lanes 5–7*) for 10 min at 25 °C followed by a 20-min 37 °C incubation. 500 nM naked 25-bp duplex competitor was added either before (*B*) or after (*A*) addition of Ku. Inferred complex composition is indicated to the left of the panel; *species I*, nucleosome; *species II*, nucleosome bound by one molecule Ku; *species III*, nucleosome bound by two molecules of Ku.

itor DNA to both remove Ku and ensure potentially displaced histones cannot be reincorporated into the nucleosome. Removal of Ku from the nucleosome restores the nucleosome to its original mobility (Fig. 6*D*), arguing against eviction of histones.

Ku Fails to Bind RAG-sequestered Signal Ends—Ku must also recognize and promote the joining of protein-occluded double strand break intermediates during V(D)J recombination, a genome rearrangement required for assembly of the mature antigen-specific receptor genes of the mammalian immune system. V(D)J recombination requires one each of the two types of targeting signals (12-RS and 23-RS) and is initiated when the RAG1 and RAG2 proteins bind this pair of signals and cleave the flanking chromosomal DNA. Importantly, RAG proteins remain in a complex with the paired signals after cleavage (paired SEC), and this complex is sufficient to block signal end joining in both extract- (35–37) and purified protein-based (26) *in vitro* assays. Nevertheless, signal end intermediates in V(D)J recombination are efficiently joined together by NHEJ in cells. We therefore utilized an EMSA to test whether Ku could directly load on RAG-bound signal ends.

We generated an SEC *in vitro* (see Fig. 7*A*) by incubating purified RAG proteins and HMG1 (high mobility group protein 1) with recombination signal-containing oligonucleotide duplexes. A stable SEC (species IV) requires RAG1, RAG2, HMG1, and both 12-RS and 23-RS to be present; this species is inefficiently formed when one of the signal sequences is omitted (Fig. 7*B*, compare *species III* and *IV*, *lanes 3* and *4*) or if one of the signals is substituted with an oligonucleotide duplex composed of irrelevant sequence.[3] We used a pair of RS-containing oligonucleotide duplexes to generate the SEC instead of a continuous DNA fragment terminating in signals ends (as is typically generated *in vivo*) because this keeps the complex sufficiently small to be resolved by EMSA. However, these duplexes possess an end distal to the site of cleavage that is anomalously accessible. We therefore selectively blocked access to these ends as described above by appending biotin to the appropriate ends of the oligonucleotides when synthesized and including streptavidin in these reactions (Fig. 7, *A* and *B*, *species V*).

Addition of Ku to SEC mixtures generates a new species (species VI) with increased mobility relative to the streptavidin-blocked SEC (species V). However, this probably reflects loading of Ku onto a minor population of incompletely formed SEC (evident as species with heterogeneous mobility in *lanes 4* through *7*) because Ku changes neither the mobility nor the intensity of accurately formed SEC (Fig. 7*B*, compare *species V in lane 5* to *species V in lane 8*). Furthermore, the mobility of species V was significantly reduced by an antibody to the maltose-binding protein tag on the RAG proteins, but not an antibody directed against Ku, excluding the possibility that Ku was present in the SEC, but our EMSA was unable to resolve this species. Accurately formed SEC similarly resisted loading of Ku when incubated for longer times (1 h), at higher temperature (37 °C), with increased salt (150 mM KCl), using either Mg^{2+} or Ca^{2+}, with higher concentrations of Ku (250 nM), or when accompanied by XRCC4-ligase IV, DNA-PKcs, and ATP.[3] Therefore, we conclude that Ku, either alone or together with core NHEJ factors, is probably insufficient to recognize and promote joining of DNA ends in the context of the SEC.

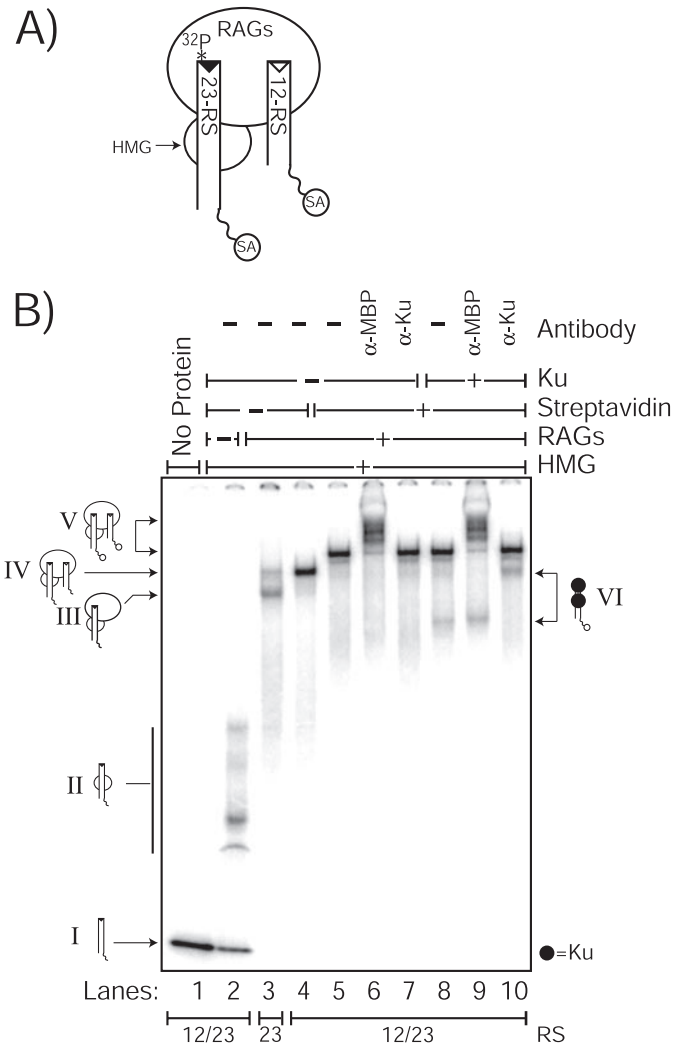

FIGURE 7. **The DNA binding activity of Ku at RAG bound signal ends.** *A*, a signal end complex is defined here as RAG1, RAG2, and HMG1 bound to two-oligonucleotide DNA duplexes, one containing the 12-RS and the other containing the 23-RS. A streptavidin-biotin complex was used to block the ends of the DNA duplexes distal to the site of cleavage. *B*, approximately 10 ng/μl of purified RAG1 and RAG2 and 425 nM HMG1 were incubated with 0.4 nM radiolabeled 23-RS-containing and 10 nM 12-RS-containing DNA fragments at 37 °C for 10 min. 5 μM streptavidin was added at 25 °C for 5 min prior to addition of 25 nM Ku. Antibody supershifts required an additional 10-min room temperature incubation step with either 0.2 μg of the monoclonal antibody to Ku or 1 μl of a polyclonal antisera recognizing the maltose binding domain fused to recombinant RAG proteins. The inferred composition of each of the generated species is indicated to the side of the panel: *species I*, 23-RS; *species II*, HMG1-bound 23-RS; *species III*, RAGs and HMG1 bound to the 23-RS; *species IV*, SEC; *species V*, streptavidin-blocked SEC (*upper arrow* indicates α-MBP supershift); *species VI*, Ku bound to incompletely formed SEC (*upper arrow* indicates α-Ku supershift).

DISCUSSION

In vitro, at least 50 bps of naked DNA are required to assemble a functional ligation complex at a DNA end (38), but DNA double strand breaks in cells are typically occluded by nucleosomes, linker histones, and other proteins involved in chromatin structure. Therefore, the ability of Ku to load onto such ends is likely a major determinant of the efficiency of cellular NHEJ given the critical place of Ku in break recognition and subsequent nucleation of the NHEJ complex.

The unusual structure of Ku, which requires DNA ends to be threaded through a circular protein channel, might argue it is poorly suited for loading on protein-occluded ends. Consistent with this argument, we show the RAG proteins bound to signal end intermediates in V(D)J recombination strongly resist the ability of Ku to recognize and load on these DNA ends. Nevertheless, NHEJ must resolve these intermediates in cells to maintain intact receptor loci in certain contexts, and it may be critical in reducing RAG-mediated transposition activity (39). The prior disassembly of the SEC by factors extrinsic to the core NHEJ machinery and the SEC (*e.g.* by proteolysis) (40–42) may thus be the limiting step in resolution of this class of protein-occluded ends.

In contrast, Ku appears readily able to displace the more weakly bound linker histone H1. Because H1 occlusion is sufficient to block activity of the NHEJ ligase (ligase IV) *in vitro* (27), this argues that the ability of Ku to recognize broken ends occluded by H1 may be the important first step in allowing NHEJ to act on breaks generated in linker regions of chromatin. However, we note linker histones may be bound more tightly in the context of higher order chromatin; thus, this question should be re-addressed when it becomes possible to accurately recapitulate higher order chromatin structures *in vitro*.

Surprisingly, Ku can also recognize DNA ends on the surface of nucleosomes and does so by the same mechanism it uses for naked DNA, threading DNA ends through its central channel. Loading of Ku can be accompanied by peeling as much as one-third of the nucleosomal DNA away from the histone octamer. However, unlike traditional chromatin remodeling, the nucleosome structure (*i.e.* octamer composition or translational position) can remain otherwise largely unperturbed and energy from ATP hydrolysis is not required. Instead, Ku presumably takes advantage of transient dissociations of DNA ("breathing") as it enters and leaves the nucleosome (43). The crystal structures of Ku bound to a DNA end (16) and the nucleosome core particle (44) also suggest Ku may be particularly well suited for loading on nucleosome-associated DNA ends as the two structures can be docked with only slight alteration of the DNA path (Fig. 8). We propose that Ku's narrow β-strand bridge portion of its DNA binding channel can act as a wedge between the DNA end and the histone octamer surface, allowing Ku to pass DNA ends through its channel while minimally disrupting histone-DNA interactions. Once bound, Ku may then translocate internally, most likely by being pushed by DNA-PKcs (29), XRCC4-Ligase IV (38), or a second molecule of Ku.

The ability of Ku to load on chromatinized ends and translocate inward may provide cells with several benefits. As suggested above, Ku alone may be sufficient for recognition of chromatinized ends and activation of NHEJ, allowing this pathway to proceed without always requiring chromatin remodeling. Alternatively, loading of Ku may be a critical first step in directing other factors to perform a limited remodeling of chromatin at ends. In yeast, Ku interacts with the SWI/SNF family remodeling complex, RSC (45, 46), and the ability of Ku to peel DNA ends from the nucleosome surface could help orient the direction of the activity of this complex such that nucleosomes are pushed away from break sites.

NHEJ thus may repair double strand breaks with minimal or no remodeling of flanking chromatin. In contrast, the other major double strand break repair pathway, homologous recom-

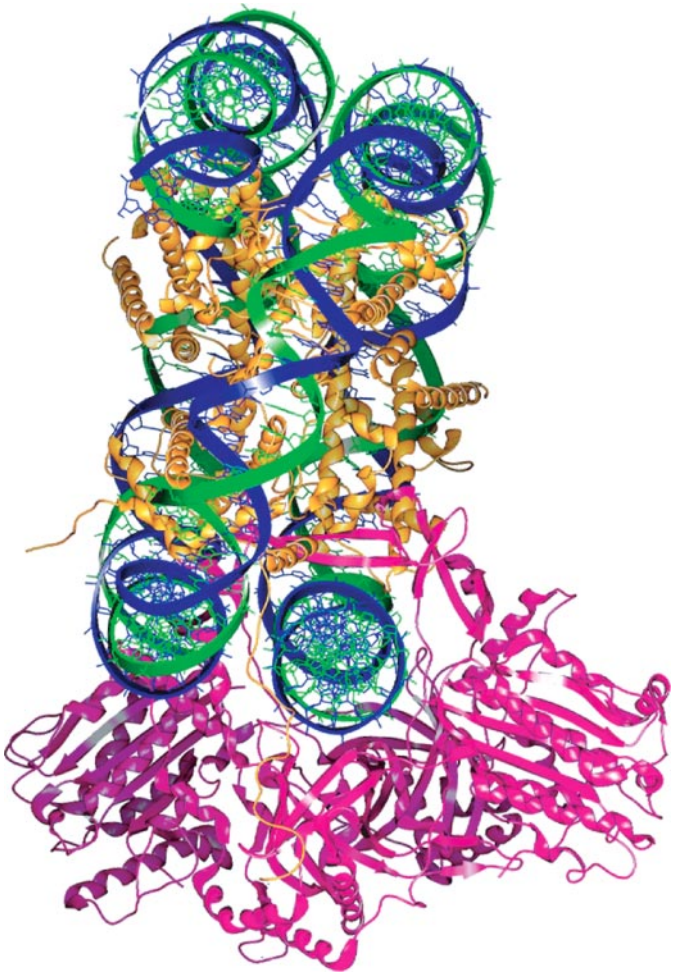

FIGURE 8. **Model of Ku bound to nucleosome-associated DNA ends.** The core nucleosome structure (Protein Data Bank accession 1AOI) and the structure of Ku bound to DNA (accession 1JEY) were docked by aligning the DNA within these structures as described under "Experimental Procedures." Ku is *magenta*, and histones are *orange*.

bination, is associated with the removal of nucleosomes within several kilobases of the break site (47). This difference may help rationalize why NHEJ is the preferred repair pathway in differentiated cells (48, 49), where significant disruption of chromatin state could lead to inappropriate gene activation.

Acknowledgments—We thank Brenda Temple (UNC) for assistance in protein modeling, the laboratory of Dr. Yi Zhang (UNC) for the gift of purified histone H1, Dr. Jonathon Widom (Northwestern University) for providing the 601.2-nucleosome positioning sequence, and members of the Ramsden laboratory for helpful discussion.

REFERENCES

1. Weterings, E., and van Gent, D. C. (2004) *DNA Repair (Amst.)* **3,** 1425–1435
2. Falzon, M., Fewell, J. W., and Kuff, E. L. (1993) *J. Biol. Chem.* **268,** 10546–10552
3. Rathmell, W. K., and Chu, G. (1994) *Mol. Cell. Biol.* **14,** 4741–4748
4. Mimori, T., and Hardin, J. A. (1986) *J. Biol. Chem.* **261,** 10375–10379
5. Paillard, S., and Strauss, F. (1991) *Nucleic Acids Res.* **19,** 5619–5624
6. Gottlieb, T. M., and Jackson, S. P. (1993) *Cell* **72,** 131–142
7. Nick McElhinny, S. A., Snowden, C. M., McCarville, J., and Ramsden, D. A. (2000) *Mol. Cell. Biol.* **20,** 2996–3003
8. Chen, L., Trujillo, K., Sung, P., and Tomkinson, A. E. (2000) *J. Biol. Chem.* **275,** 26196–26205
9. Mahajan, K. N., Nick McElhinny, S. A., Mitchell, B. S., and Ramsden, D. A. (2002) *Mol. Cell. Biol.* **22,** 5194–5202
10. Ma, Y., Lu, H., Tippin, B., Goodman, M. F., Shimazaki, N., Koiwai, O., Hsieh, C. L., Schwarz, K., and Lieber, M. R. (2004) *Mol. Cell* **16,** 701–713
11. Zhu, C., Bogue, M. A., Lim, D. S., Hasty, P., and Roth, D. B. (1996) *Cell* **86,** 379–389
12. Gu, Y., Seidl, K. J., Rathbun, G. A., Zhu, C., Manis, J. P., van der Stoep, N., Davidson, L., Cheng, H. L., Sekiguchi, J. M., Frank, K., Stanhope-Baker, P., Schlissel, M. S., Roth, D. B., and Alt, F. W. (1997) *Immunity* **7,** 653–665
13. Smider, V., Rathmell, W. K., Lieber, M. R., and Chu, G. (1994) *Science* **266,** 288–291
14. Taccioli, G. E., Gottlieb, T. M., Blunt, T., Priestley, A., Demengeot, J., Mizuta, R., Lehmann, A. R., Alt, F. W., Jackson, S. P., and Jeggo, P. A. (1994) *Science* **265,** 1442–1445
15. Yoo, S., Kimzey, A., and Dynan, W. S. (1999) *J. Biol. Chem.* **274,** 20034–20039
16. Walker, J. R., Corpina, R. A., and Goldberg, J. (2001) *Nature* **412,** 607–614
17. Schnitzler, G. (2000) in *Current Protocols in Molecular Biology* (Ausubel, F. M., Brent, R., Kingston, R. E., Moore, D. D., Seidman, J. G., Smith, J. A., and Struhl, K., eds) pp. 21.5-1–21.5-12, John Wiley and Sons, Inc., New York
18. McBlane, J. F., van Gent, D. C., Ramsden, D. A., Romeo, C., Cuomo, C. A., Gellert, M., and Oettinger, M. A. (1995) *Cell* **83,** 387–395
19. Anderson, J. D., Lowary, P. T., and Widom, J. (2001) *J. Mol. Biol.* **307,** 977–985
20. Anderson, J. D., and Widom, J. (2000) *J. Mol. Biol.* **296,** 979–987
21. Hayes, J. J., and Lee, K. M. (1997) *Methods* **12,** 2–9
22. Dyer, P. N., Edayathumangalam, R. S., White, C. L., Bao, Y., Chakravarthy, S., Muthurajan, U. M., and Luger, K. (2004) *Methods Enzymol.* **375,** 23–44
23. Blier, P. R., Griffith, A. J., Craft, J., and Hardin, J. A. (1993) *J. Biol. Chem.* **268,** 7594–7601
24. Schwanbeck, R., Xiao, H., and Wu, C. (2004) *J. Biol. Chem.* **279,** 39933–39941
25. Christopher, J. A. (2004) *SPOCK: The Structural Properties Observation and Calculation Kit (Program Manual)*, The Center for Macromolecular Design, Texas A&M University, College Station, TX
26. Jones, J. M., and Gellert, M. (2001) *Proc. Natl. Acad. Sci. U. S. A.* **98,** 12926–12931
27. Kysela, B., Chovanec, M., and Jeggo, P. A. (2005) *Proc. Natl. Acad. Sci. U. S. A.* **102,** 1877–1882
28. Park, E. J., Chan, D. W., Park, J. H., Oettinger, M. A., and Kwon, J. (2003) *Nucleic Acids Res.* **31,** 6819–6827
29. Yoo, S., and Dynan, W. S. (1999) *Nucleic Acids Res.* **27,** 4679–4686
30. Wagner, J. P., Quill, D. M., and Pettijohn, D. E. (1995) *J. Biol. Chem.* **270,** 7394–7398
31. Wisniewski, J. R., and Schulze, E. (1994) *J. Biol. Chem.* **269,** 10713–10719
32. Namsaraev, E. A., and Berg, P. (1998) *J. Biol. Chem.* **273,** 6177–6182
33. de Vries, E., van Driel, W., Bergsma, W. G., Arnberg, A. C., and van der Vliet, P. C. (1989) *J. Mol. Biol.* **208,** 65–78
34. Ma, Y., and Lieber, M. R. (2001) *Biochemistry* **40,** 9638–9646
35. Ramsden, D. A., Paull, T. T., and Gellert, M. (1997) *Nature* **388,** 488–491
36. Weis-Garcia, F., Besmer, E., Sawchuk, D. J., Yu, W., Hu, Y., Cassard, S., Nussenzweig, M. C., and Cortes, P. (1997) *Mol. Cell. Biol.* **17,** 6379–6385
37. Agrawal, A., and Schatz, D. G. (1997) *Cell* **89,** 43–53
38. Kysela, B., Doherty, A. J., Chovanec, M., Stiff, T., Ameer-Beg, S. M., Vojnovic, B., Girard, P. M., and Jeggo, P. A. (2003) *J. Biol. Chem.* **278,** 22466–22474
39. Reddy, Y. V., Perkins, E. J., and Ramsden, D. A. (2006) *Genes Dev.* **20,** 1575–1582
40. Jones, J. M., and Gellert, M. (2003) *Proc. Natl. Acad. Sci. U. S. A.* **100,** 15446–15451
41. Lee, J., and Desiderio, S. (1999) *Immunity* **11,** 771–781
42. Yurchenko, V., Xue, Z., and Sadofsky, M. (2003) *Genes Dev.* **17,** 581–585
43. Li, G., Levitus, M., Bustamante, C., and Widom, J. (2005) *Nat. Struct. Mol.*

Biol. **12,** 46–53
44. Luger, K., Mader, A. W., Richmond, R. K., Sargent, D. F., and Richmond, T. J. (1997) *Nature* **389,** 251–260
45. Shim, E. Y., Ma, J. L., Oum, J. H., Yanez, Y., and Lee, S. E. (2005) *Mol. Cell. Biol.* **25,** 3934–3944
46. Shim, E. Y., Hong, S. J., Oum, J. H., Yanez, Y., Zhang, Y., and Lee, S. E. (2006) *Mol. Cell. Biol.* **5,** 1602–1613
47. Tsukuda, T., Fleming, A. B., Nickoloff, J. A., and Osley, M. A. (2005) *Nature* **438,** 379–383
48. Gao, Y., Sun, Y., Frank, K. M., Dikkes, P., Fujiwara, Y., Seidl, K. J., Sekiguchi, J. M., Rathbun, G. A., Swat, W., Wang, J., Bronson, R. T., Malynn, B. A., Bryans, M., Zhu, C., Chaudhuri, J., Davidson, L., Ferrini, R., Stamato, T., Orkin, S. H., Greenberg, M. E., and Alt, F. W. (1998) *Cell* **95,** 891–902
49. Clejan, I., Boerckel, J., and Ahmed, S. (2006) *Genetics* **173,** 1301–1317